THE JOURNAL OF PHYSICAL CHEMISTRY A
A JOURNAL OF THE AMERICAN CHEMICAL SOCIETY

pubs.acs.org/JPCA Article

Reworking the Tao–Mo Exchange–Correlation Functional. III. Improved Deorbitalization Strategy and Faithful Deorbitalization

Published as part of The Journal of Physical Chemistry A virtual special issue "Gustavo Scuseria Festschrift".

H. Francisco,* A. C. Cancio, and S. B. Trickey*

Cite This: *J. Phys. Chem. A* 2024, 128, 6010–6018 Read Online

ACCESS | Metrics & More | Article Recommendations | Supporting Information

ABSTRACT: We present a deorbitalization of the recent simplified, regularized Tao–Mo exchange functional (*J. Chem. Phys.* **2023**, *159*, 214102) that is faithful to the parent functional. That is a major gain relative to our earlier deorbitalization which did poorly on molecular heats of formation (*J. Chem. Phys.* **2023**, *159*, 214103). The improvement arises from augmentation of the Mejía-Rodríguez and Trickey deorbitalization strategy (*Phys. Rev. A* **2017**, *96*, 052512) to use a smoothed replacement for the reduced density Laplacian (conventionally denoted q) obtained from that Laplacian itself. The augmentation also rationalizes the improvement obtained from the cutoff of $q < 0$ that was poorly understood at the time of the previous paper. The new scheme yields deorbitalized chemical region indicators that are much closer to those from the parent, orbital-dependent functional than were obtainable from the previous deorbitalization. It also replicates the good 3d elemental magnetization of the parent functional reasonably well.

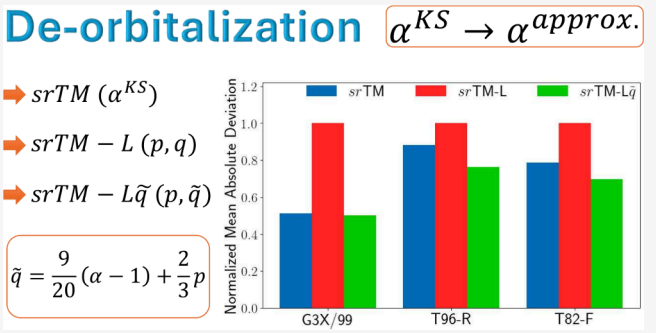

CONTEXT

In the second of the two preceding papers in this series[1,2] ("Paper II" hereafter) we studied the deorbitalization of the simplified regularization of the Tao–Mo exchange functional (called *sreg*TM) given in the first paper, "Paper I" hereafter. We focus here on the version called *v2-sreg*TM. To avoid worsening cumbersome notation, here we denote it simply as *sr*TM.

We found that straightforward application of the Mejía-Rodríguez and Trickey (hereafter "M-RT") deorbitalization strategy[3,4] did not work well but that *sr*TM could be deorbitalized with nontrivial loss of fidelity to the parent functional by use of a rather peculiarly parametrized version of the previously used deorbitalizer. We also mentioned an even more peculiar deorbitalization that reproduced most error patterns on the usual molecular and solid test sets but that apparently depended upon cancellation of large errors introduced by deorbitalization of the indicator functions α and z_{rev} (definitions below). Therefore, we did *not* recommend that second peculiar deorbitalization.

Here we resolve those issues by introducing a substantive augmentation of the M-RT approach. Some definitions are needed to proceed. The exchange–correlation (XC) functionals of interest are meta-generalized gradient approximations (meta-GGAs). Generically, the exchange (X) term is in terms of the enhancement factor F_x and associated variables

$$E_x^{mGGA}[n] = c_x \int \mathrm{d}\mathbf{r}\, n^{4/3}(\mathbf{r})\, F_x(s[n(\mathbf{r})],\, \tau_s(\mathbf{r})) \tag{1}$$

$$s := \frac{|\nabla n(\mathbf{r})|}{2(3\pi^2)^{1/3} n^{4/3}(\mathbf{r})} \tag{2}$$

$$\tau_s := \frac{1}{2}\sum_i f_i\, |\nabla \varphi_i(\mathbf{r})|^2 \tag{3}$$

with the electron number density $n(\mathbf{r}) = \sum_i f_i |\varphi_i(\mathbf{r})|^2$ from the Kohn–Sham (or generalized K–S) orbitals and $c_x := -\frac{3}{4}\left(\frac{3}{\pi}\right)^{1/3}$. Note that here and throughout, as in Papers I and II, we treat the un-spin-polarized case explicitly. As with those papers and the original Tao–Mo formulation, we assume that the spin-polarized case is obtained from exact spin-scaling.[5]

The task of deorbitalization is to replace the explicitly orbital- and occupation-number-dependent τ_s with a pure density functional dependent at most (for reasons of numerical

Received: April 22, 2024
Revised: June 17, 2024
Accepted: June 27, 2024
Published: July 12, 2024

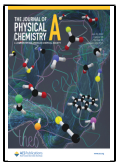

https://doi.org/10.1021/acs.jpca.4c02635
J. Phys. Chem. A 2024, 128, 6010–6018

tractability) upon $n(\mathbf{r})$, ∇n, and $\nabla^2 n$. Detailed motivation for deorbitalization and a sketch of the history of the approach are in Paper II.

The orbital dependence of most meta-GGA X functionals comes through iso-orbital indicators, of which the most widely used (though not the only one; see below) is

$$\alpha[\{\varphi\}] := \frac{\tau_s - \tau_W}{\tau_{TF}} \tag{4}$$

with

$$\tau_{TF} := c_{TF} n^{5/3}(\mathbf{r}) \tag{5}$$

$$\tau_W := \frac{1}{8}\frac{|\nabla n(\mathbf{r})|^2}{n(\mathbf{r})} \tag{6}$$

being the Thomas−Fermi and von Weizsäcker KE densities respectively and $c_{\mathrm{TF}} := \frac{3}{10}(3\pi^2)^{2/3}$.

M-RT gave a systematic strategy for replacement of τ_s.[3,4,6] One selects a promising approximate kinetic energy density (KED), $\tau[n, \nabla n, \nabla^2 n] \approx \tau_s[n]$, and adjusts the parameters in it so as to give a good approximation to α on nonbonded systems (e.g., atoms),

$$\alpha_L[n, \nabla n, \nabla^2 n] \approx \alpha[\{\varphi\}] \tag{7}$$

Here and throughout the subscript "L" denotes a density-Laplacian-dependent quantity.

The various Tao−Mo forms[7−10] use a second chemical region indicator as well. The original version

$$z := \frac{\tau_W}{\tau_s} \equiv \frac{5p}{5p + 3\alpha} \tag{8}$$

(with $p := s^2$ and s given by eq 2) is well-known to be problematic, suffering from order-of-limits inconsistency as both α and $p \to 0$. It is replaced in our *sr*TM by the simple, physically consistent regularization

$$z_{rev}(\alpha, p) = \frac{5p + \epsilon_p}{5p + 3\alpha + \epsilon_p} \tag{9}$$

with $\epsilon_p = 0.5$. The detailed discussion of this regularization and its effect on electronic structure prediction are given in Paper I.

The obvious use of the M-RT strategy is to deorbitalize z_{rev} by substitution of α_L. The essential finding from Paper II is that this fails. In particular, it gives very poor mean absolute deviation (MAD) for molecular heats of formation as tested on the G3/99 data set,[11,12] 23.96 kcal/mol versus 5.985 kcal/mol for the parent *sr*TM meta-GGA. But an unconventional optimization (cutoff of negative $\nabla^2 n$ contributions) of the Perdew−Constantin KED parameters[3,13] was reasonably successful, *except* for molecular heat of formation MAD. That "PC_{rep}" parametrization gave 11.471 kcal/mol, much improved but still poor (≈90% larger than from the parent *sr*TM). The MAD comparison for solid cohesive energies, on the other hand, was much better: 0.216 eV/atom for the parent vs 0.205 eV/atom for the deorbitalized version. Based on the errors in atomic total energies and molecular total energies, we conjectured that the problem with the molecular heat of formation MAD arose from lack of the same beneficial cancellation of error (between molecules and constituent atoms) for the deorbitalized and parent functionals. An unresolved puzzle was that use of the $\nabla^2 n < 0$ cutoff in the functional itself as well as in PC_{rep} improved the MADs further but the deorbitalized α and z_{rev} were manifestly quite wrong.

That is the setting. In what follows, we analyze the unconventional parametrization. Motivated by that, then we introduce a novel way to utilize the reduced density Laplacian variable q (defined below at eq 10) by using it to deorbitalize a gradient-expansion approximation to itself. We report numerical results on standard molecular and solid test sets that verify that the new deorbitalization replicates the performance of the parent functional *sr*TM; i.e., it is a faithful deorbitalization. This includes reasonable preservation of elemental 3d magnetization. We also compare the number of SCF steps and time per step for the parent and faithfully deorbitalized versions.

COMPUTATIONAL DETAILS

Note that, throughout, the calculations on molecules and solids reported here were done with the codes, basis sets, projector augmented wave data sets (PAWs), and control parameters described in Section IV.A of Paper I. The molecular and solids test sets used here are the same as in refs 1 and 2, which are the following: molecular heats of formation by Curtiss et al.[11,12] for the 223 molecules of the G3X/99 test set, the T96-R test set[14,15] to study the bond lengths, and the T82-F[14,15] test set for the harmonic vibrational frequencies, and for solids, the static-crystal lattice constants and cohesive energies for 55 solids,[16] moduli bulk for 44 solids,[17] and Kohn−Sham band gaps of 21 insulators and semiconductors.[18]

INSIGHTS FROM PECULIAR DEORBITALIZATION

The M-RT deorbitalizers[3,4,6] depend on p and the reduced density Laplacian

$$q := \frac{\nabla^2 n}{4(3\pi^2)^{2/3} n^{5/3}} \tag{10}$$

Though the PC_{opt} form originated as the Perdew−Constantin approximation[13] to the Pauli kinetic energy,[19] it is reparametrized against $\alpha[\{\varphi\}]$ values for the parent functional on the first 18 neutral atoms (in the central field approximation) to improve satisfaction of eq 7. That is denoted by "opt".

As already intimated, for the molecular heats of formation, that procedure did not provide a satisfactory deorbitalization of *sr*TM. The spiky singularity of q at nuclear sites led to the discovery that a sharp cutoff of q, namely, $q \to q_H$, with

$$q_H := qH(q) \tag{11}$$

and $H(q)$ the Heaviside step function gave the somewhat more successful parametrization denoted PC_{rep}. The $q \geq 0$ constraint was used only in optimization of parameters, not in the actual deorbitalizer.

Given that inconsistency in the PC_{rep} procedure, it was inescapable to try the q_H cutoff consistently, in the deorbitalization itself. We label that version as $\mathrm{PC}_{rep}(q_H)$. It was discussed briefly in Section IV of Paper II as the "brutal approximation". Comparative results are in Tables 1 and 2. (Aside: For the parent meta-GGA functional, the band gap data in Table 2 and later counterpart tables are from generalized Kohn−Sham calculations. Results for deorbitalized functionals are from ordinary KS calculations.) All of the molecular MADs are improved compared to the simple (inconsistent) PC_{rep} values. The solid system MADs are the same or slightly worsened.

https://doi.org/10.1021/acs.jpca.4c02635
J. Phys. Chem. A 2024, 128, 6010−6018

Table 1. Molecular Test Results Summary for the Plain M-RT Deorbitalized Versions, *sr*TM-L, of the *sr*TM XC Functional with the PC_{rep} Deorbitalizer, for Parametrization Only and in the "Brutal Approximation" (See Text)[a]

		*sr*TM	*sr*TM-L (PC_{rep})	*sr*TM-L ($PC_{rep}(q_H)$)
Heats of Formation	ME	−3.512	8.675	−2.875
	MAD	5.895	11.471	7.702
Bonds	ME	0.013	0.014	0.009
	MAD	0.015	0.017	0.014
Frequencies	ME	−19.275	−32.277	−11.776
	MAD	34.272	43.499	30.606

[a]Numerical techniques as in Paper II. Heat of formation errors in kcal/mol, bond length errors in Å, and frequency errors in cm^{-1}. "ME" is mean error, "MAD" is mean absolute deviation.

Table 2. As in Table 1 for Solid Test Sets[a]

		*sr*TM	*sr*TM-L(PC_{rep})	*sr*TM-L($PC_{rep}(q_H)$)
Lattice Constants	ME	0.004	0.018	0.020
	MAD	0.031	0.041	0.040
Cohesive Energies	ME	0.159	0.010	0.080
	MAD	0.216	0.205	0.218
Bulk Moduli	ME	0.223	−3.265	−4.000
	MAD	6.602	8.747	9.066
KS Band Gaps	ME	−1.53	−1.73	−1.73
	MAD	1.53	1.73	1.73

[a]Equilibrium lattice constant errors in Å, cohesive energy errors in eV/atom, bulk modulus errors in GPa, and Kohn−Sham (and generalized K−S) band gap errors in eV.

Even so, the molecular heat of formation MAD for the brutal approximation deorbitalization still is unsatisfactory, 30% larger than for the parent. Worse, from the perspectives of reliability and interpretation, is the misbehavior of the indicator functions. As noted in Paper II, both the α_{L-MRT} and $z_{rev,L-MRT}$ for the $PC_{rep}(q_H)$ deorbitalization are qualitatively quite different from the corresponding functions for the parent functional.

To get rid of any sharp cutoff effects, we studied M-RT deorbitalization in combination with a smoothly truncated version of q,

$$q_s := q\sigma(q, q_0) \tag{12}$$

with the sigmoid cutoff

$$\sigma(q, q_0) = \frac{1}{1 + \exp(-a_s(q + q_0))} \tag{13}$$

The value $q_0 = 0$ gives a smooth cutoff of essentially all $q < 0$, whereas $q_0 > 0$ provides introduction of adjustable regions of $q < 0$. The parameter a_s was determined by making $q_s(q_0 = 0)$ as similar as possible to q for the atomic hydrogen density. The result is $a_s = 11.3307$. Figure 1 shows the fit. The rationale for calibrating to the H density is straightforward. For physical densities, negative values of q occur in the neighborhoods of nuclear sites. From the Kato cusp condition[20−23] the density in a suitably small neighborhood of a nucleus with charge Z is proportional to $\exp(-2Zr)$, thus $q \propto -Z/r$ in that neighborhood. In construction of TM-type functionals (specifically, the F_x^{DME} term; see eqs 7−12 of ref 1), recovery of the atomic H exchange energy is an enforced constraint, so

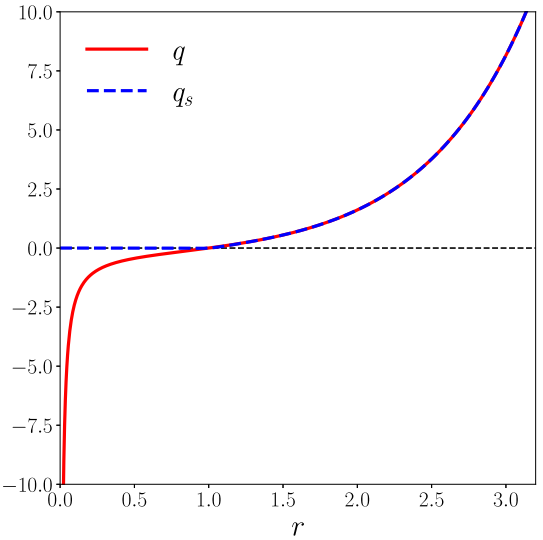

Figure 1. q and $q_s(q_0 = 0)$ for the atomic hydrogen density. The fit value $a_0 = 11.3307$.

it is consistent to choose $Z = 1$ to calibrate the sigmoidal cutoff of q.

With this $q_s(q_0)$, we redid the calculations with the PC_{rep} parametrization. To distinguish these exploratory deorbitalizations from those obtained with the basic M-RT procedure, we denote these deorbitalizations as *sr*TM-$L_{MRT}(PC_{rep}(p, q_s))$. What Tables 3 and 4 show unequivocally is that even $q_0 = 1$ is

Table 3. Effects of Using $q_s(q_0)$ in Combination with M-RT Deorbitalization: Molecular Test Set Results for Deorbitalized *sr*TM-L_{MRT} Using PC_{rep} (p, q_s) as Deorbitalizer with Different q_0 Values[a]

		*sr*TM-$L_{MRT}(PC_{rep}(p, q_s))$			
		$q_0 = 0.0$	$q_0 = 1.0$	$q_0 = 2.0$	$q_0 = 3.0$
Heats of Formation	ME	−3.232	8.690	8.668	8.684
	MAD	7.614	11.473	11.472	11.474
Bonds	ME	0.016	0.014	0.014	0.014
	MAD	0.016	0.017	0.017	0.017
Frequencies	ME	−32.146	−32.418	−32.368	−26.186
	MAD	42.541	43.666	43.581	49.486

[a]Heat of formation errors in kcal/mol, bond length errors in Å, and frequency errors in cm^{-1}.

Table 4. As in Table 3 for Solid Test Sets[a]

		*sr*TM-$L_{MRT}(PC_{rep}(p,q_s))$			
		$q_0 = 0.0$	$q_0 = 1.0$	$q_0 = 2.0$	$q_0 = 3.0$
Lattice Constants	ME	0.017	0.016	0.017	0.016
	MAD	0.040	0.039	0.040	0.040
Cohesive Energies	ME	0.075	0.005	0.011	−0.002
	MAD	0.216	0.202	0.207	0.194
Bulk Modulus	ME	−3.174	−3.282	−3.408	−3.280
	MAD	8.602	8.630	8.679	8.729
Band Gaps	ME	−1.69	−1.73	−1.73	−1.73
	MAD	1.69	1.73	1.73	1.73

[a]Equilibrium lattice constant errors in Å, cohesive energy errors in eV/atom, bulk modulus errors in GPa, and Kohn−Sham band gap errors in eV.

https://doi.org/10.1021/acs.jpca.4c02635
J. Phys. Chem. A 2024, 128, 6010−6018

enough to cause substantial worsening of the molecular heat of formation MAD with respect to the result for $q_0 = 0$, without causing any worsening of the other molecular metrics. The solid metrics actually get a little better with $q_0 = 1$.

We emphasize that the $q_s(q_0 = 0)$ heat of formation MAD still is unsatisfactory, almost 30% larger than for the parent, essentially the same as for the brutal approximation. For the r^{2}SCAN[24] functional, in contrast, the parent MAD is 4.49 kcal/mol while the M-RT deorbitalization, r^{2}SCAN-L, gives 5.30 kcal/mol, 18% larger.[6] Worse, Figure 2 shows the price of

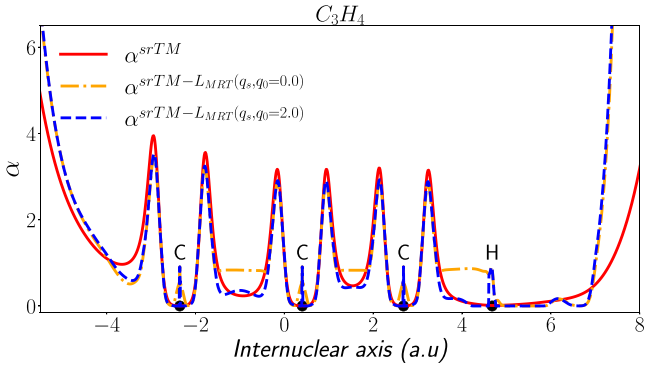

Figure 2. Orbital-dependent α from *sr*TM and its deorbitalized approximations from $PC_{rep}(p,q_s)$ for the C_3H_4 molecule for two q_0 values. The plots are along the molecular axis.

using $q_0 = 0$. It confirms the peculiar behavior of the deorbitalized indicator functions mentioned earlier and in Paper II. Specifically $\alpha_{L-MRT}(q_s, q_0 = 0)$ is qualitatively different from the parent (orbital-dependent) α in each bonding region. The C−H bond is instructive. A value of $q_0 = 1$ or higher is required to get an α_{L-MRT} that resembles, at least roughly, the parent α. But that q_0 value degrades the heat of formation MAD severely.

Thus, a simple smooth cutoff of $q < 0$ is not enough to rescue M-RT deorbitalization of *sr*TM. The choice $q_0 = 0$ clearly biases α_{L-MRT} to inauthentic values (relative to the parent functional) that yield a fortuitous reduction in heat of formation MAD. There are changes in molecular frequencies only for $q_0 = 3$, while more serious errors occur in heat of formation for smaller q_0. Setting $q_0 = 0$ resolves both issues. The details of how that occurs are obscure because of the complicated *sr*TM form. Without going into belabored investigation, what is clear is that the cutoff has altered some of the physics in the KE density approximation used as a deorbitalizer. The competing effects of allowing or disallowing $q < 0$ show that the deorbitalization needs more flexibility. The specific task is to devise a better treatment of q, one that achieves the benefits of the non-negativity of $q_s(q_0 = 0)$ but without the limitations caused by its arbitrariness.

DEORBITALIZED LAPLACIAN

Though unrecognized at the time, Paper II in fact indicated a way forward. In the Tao−Mo variants, including *sr*TM, the reduced Laplacian q appears without any connection with deorbitalization. To avoid the effects of divergences of q at nuclear sites for densities with a true Kato cusp (and spiky behavior for cusps represented in a finite Gaussian basis), q is replaced in Tao−Mo variants with

$$\tilde{q}(\alpha, p) := \frac{9}{20}(\alpha - 1) + \frac{2}{3}p \tag{14}$$

See eq 18 in Paper I. Because it is obtained from an approximation to the gradient expansion, this smooth variable approaches q for slowly varying densities.

Paper II had suggested that what might be needed was "... reproduction of the behavior of $\tilde{q}(\alpha, p)$ with a function of p and q." There also was discussion of the oddity that M-RT deorbitalization replaces the orbital-dependent α with a q-dependent approximation, $\alpha_{L,MRT}(p, q)$, which led to the seeming circularity of $\tilde{q}(\alpha_{L,MRT}(p, q), p)$, that is, an approximation to q that depends upon itself. As Figure 4 of Paper II illustrated, the result was a smooth approximation. For positive q, $\tilde{q}(\alpha_{L,MRT}(p, q), p)$ is very close to q but has only a small negative region compared to the original q.

What had not been discussed was the evident incompatibility with the basic TM structure introduced by the M-RT deorbitalization. It results in having both $\tilde{q}$ and a bare q dependence in the deorbitalized form of the $F_x^{sc}(p, \alpha)$ term in the TM exchange. That term is

$$F_x^{sc}(p, \alpha) := \left\{1 + 10\left[\left(\frac{10}{81} + \frac{50}{729}p\right)p + \frac{146}{2025}\tilde{q}^2 - \frac{73}{405}\tilde{q}\frac{3z_{rev}}{5}(1 - z_{rev})\right]\right\}^{1/10} \tag{15}$$

Notice that M-RT deorbitalization of z_{rev} introduces a plain q dependence, even though such dependence explicitly was removed in the construction[7] of F_x^{sc} by use of $\tilde{q}$. This is precisely the "circularity" mentioned above.

Upon reflection it becomes apparent that it would be more nearly consistent to augment M-RT deorbitalization to include replacement of q by a $\tilde{q}_L$ constructed from a $\tilde{q}$ version of the M-RT α_L. Put another way, the approach is to deorbitalize $\tilde{q}$ into $\tilde{q}_L$ and subsequently replace q in eq 15 by $\tilde{q}_L$. The inherently nested or recursive character of this approach forces a design choice. We investigated what appear to be the two simplest possible schemes. Both use two deorbitalizations done with the chosen approximation. Described stepwise, "Scheme 1" is the following procedure.

1. Start with a model for α, indicated by KEDF (kinetic energy density functional). Get an initial M-RT deorbitalization $\alpha_{L,0}$:

$$\alpha_{L,0}(p, q) := \alpha^{KEDF}(p, q) \tag{16}$$

2. Then construct an orbital-independent version of $\tilde{q}$:

$$\tilde{q}_{L,0}(p, q) := \tilde{q}(\alpha_{L,0}(p, q), p) \tag{17}$$

3. Then construct a second deorbitalized α:

$$\alpha_L(p, q) := \alpha^{KEDF}(p, \tilde{q}_{L,0}(p, q)) \tag{18}$$

4. From that, construct the deorbitalized $\tilde{q}$ that is used, namely

$$\tilde{q}_L(p, q) := \tilde{q}(\alpha_L(p, q), p) \tag{19}$$

"Scheme 2" differs only in that the last step, construction of $\tilde{q}_L(p, \tilde{q}_{L,0})$, is omitted. Instead, $\tilde{q}_{L,0}$ and α_L are used.

https://doi.org/10.1021/acs.jpca.4c02635
J. Phys. Chem. A 2024, 128, 6010−6018

Table 5. Molecular Test Set Results for the Parent *sr*TM XC Functional, the Original Deorbitalization, and the Different M-RT-$\tilde{q}$ Deorbitalized Versions *sr*TM-L$\tilde{q}$[a]

				*sr*TM-L$\tilde{q}$			
		*sr*TM[1]	*sr*TM-L,PC_{rep}[2]	PC_{rep}		PC_{opt}	
			(*p*,*q*)	Scheme 1	Scheme 2	Scheme 1	Scheme 2
Heats of Formation	ME	−3.512	8.675	−6.815	−5.416	0.313	2.451
	MAD	5.895	11.471	7.864	6.647	5.770	6.265
Bonds	ME	0.013	0.014	0.003	0.004	0.011	0.012
	MAD	0.015	0.017	0.010	0.010	0.013	0.014
Frequencies	ME	−19.275	−32.277	−0.472	−2.301	−20.550	−23.583
	MAD	34.272	43.491	29.992	29.883	36.360	37.720

[a]Heat of formation errors in kcal/mol, bond length errors in Å, and frequency errors in cm^{-1}.

Table 6. Comparison of Solid System Errors for Density Functional Approximation Combinations as in Table 5 for Four Solid Test Sets[a]

				*sr*TM-L$\tilde{q}$			
		*sr*TM[1]	*sr*TM-L PC_{rep}[2]	PC_{rep}		PC_{opt}	
			(*p*,*q*)	Scheme 1	Scheme 2	Scheme 1	Scheme 2
Lattice constants	ME	0.004	0.018	0.005	0.007	0.009	0.011
	MAD	0.031	0.041	0.040	0.041	0.043	0.044
Cohesive energies	ME	0.159	0.010	−0.076	−0.077	−0.017	−0.035
	MAD	0.216	0.205	0.236	0.232	0.186	0.179
Bulk moduli	ME	0.223	−3.265	−2.974	−3.208	−3.507	−3.988
	MAD	6.602	8.747	8.670	8.455	8.583	9.057
Band Gaps	ME	−1.53	−1.73	−1.56	−1.56	−1.62	−1.63
	MAD	1.53	1.73	1.56	1.56	1.62	1.63

[a]Equilibrium lattice constant errors in Å, cohesive energy errors in eV/atom, bulk modulus errors in GPa, and Kohn−Sham (and generalized K−S) band gap errors in eV.

Please note. For clarity, in what follows we denote the augmented M-RT approach as "M-RT-$\tilde{q}$". The deorbitalized quantities and results from M-RT-$\tilde{q}$ are denoted with the tag or the subscript $L\tilde{q}$. Though clumsy, it is essential to emphasize the difference introduced by the recursive use of $\tilde{q}$.

As to the parameters themselves, what is evident from Paper II is that detailed differences in parametrization do not change the values in the PC form much. The only large shift is from use of q to use of q_H. When we used the smoothly truncated q_s, reparametrizing PC did not improve the results compared to those from the PC_{rep} parameters. Recall also that Paper II showed that the PC_{rep} parameters yield a quite good reproduction of $\tilde{q}_{L,0}$. We have observed the same with PC_{opt} parameters. For clarity of comparison as well simplicity, therefore, we kept the two sets, PC_{opt} (a = 1.78472 and b = 0.25830) and PC_{rep} (a = 1.50440 and b = 0.61565).

For molecules and solids respectively, Tables 5 and 6 present the outcomes of M-RT-$\tilde{q}$ deorbitalization with the two schemes for the two sets of parameters. The improved performance relative to all the previous deorbitalization attempts is evident, especially for the three molecular test sets. Employment of the deorbitalizer PC_{rep} in both schemes gives notable enhancement in MADs for the bonds and frequencies test sets. For PC_{opt} with Scheme 1, the MAD for the molecular heats of formation is slightly better than that of the parent functional. Scheme 2 also exhibits good performance for this set.

In the solids test sets, with one notable exception, there is not a major improvement in MAD for any of the properties. But the solid MADs were not a problem, so preserving them is a success. The notable exception is the improved cohesive energy MAD for either Scheme 1 or Scheme 2 in combination with PC_{opt}. Overall, it is evident that deorbitalization of the *sr*TM functional with the M-RT-$\tilde{q}$ strategy is successful, at least so far as MADs are concerned. It remains to verify that the deorbitalized chemical indicators it gives resemble their parent forms closely and that the magnetization behavior of the parent exchange−correlation functional, *sr*TM, is preserved.

Figures 3 through 10 illustrate the local behavior of $\alpha_{L\tilde{q}}$, $z_{rev,\,L\tilde{q}}$, $w(z_{rev})$, and $\tilde{q}_{L\tilde{q}}$ for the BeH and C_3H_4 (propyne) molecules. Specifically, BeH is an open-shell diatomic molecule with simple bonding, while C_3H_4 is a more complex organic molecule with multiple atoms and several types of bonds and functional groups. The two molecules thus contain a variety of

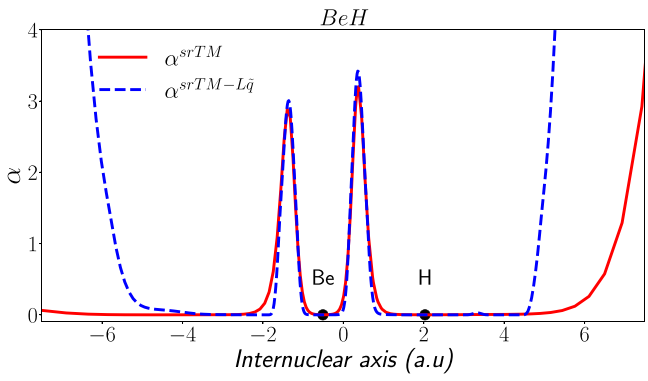

Figure 3. Orbital-dependent α and its deorbitalized approximation $\alpha_{L\tilde{q}}$ from Scheme 1 with PC_{opt} for the BeH molecule. The plot is along the molecular axis.

https://doi.org/10.1021/acs.jpca.4c02635
J. Phys. Chem. A 2024, 128, 6010−6018

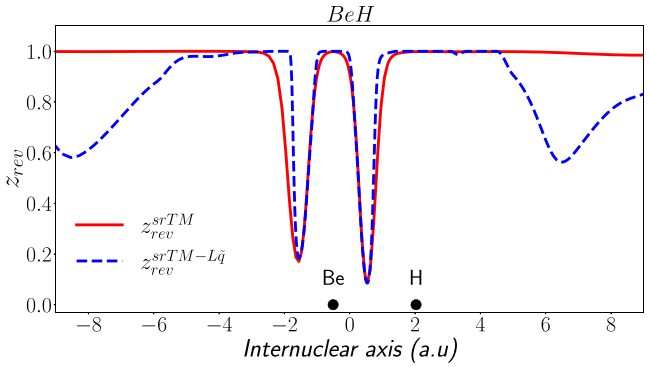

Figure 4. Orbital-dependent z_{rev} and its deorbitalized approximation from Scheme 1 with PC_{opt} for the BeH molecule. The plot is along the molecular axis.

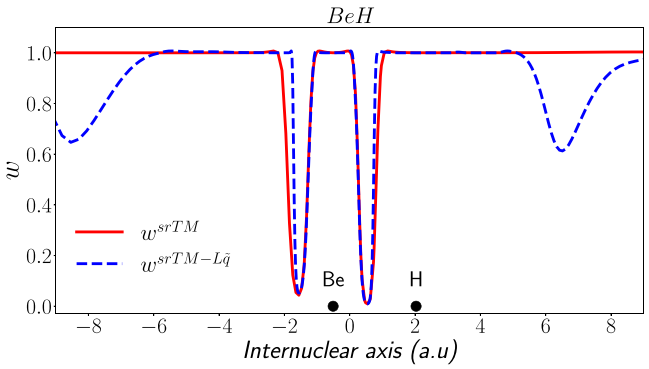

Figure 5. Orbital-dependent $w(z_{rev})$ and its deorbitalized approximation from Scheme 1 with PC_{opt} for the BeH molecule. The plot is along the molecular axis.

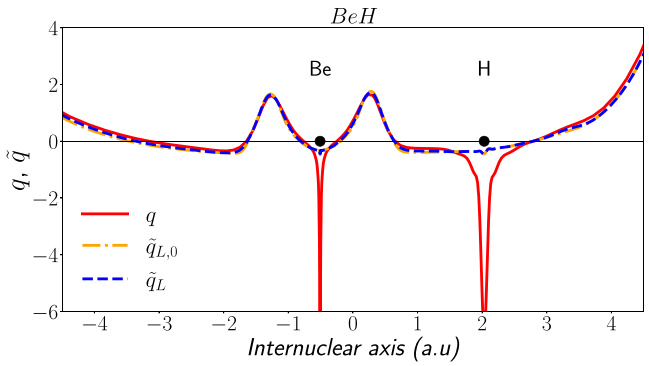

Figure 6. Reduced density Laplacian, q, and deorbitalized $\tilde{q}$ from Scheme 1 using PC_{opt} for the BeH molecule. The plot is along the molecular axis.

bonding types with distinct structural and electronic properties, and therefore provide a quick but representative sample of molecular bonding effects. Recall that the TM switching function is

$$w(z_{rev}) := \frac{z_{rev}^2 + 3z_{rev}^3}{(1 + z_{rev}^3)^2} \tag{20}$$

Clearly the M-RT-$\tilde{q}$ protocol does preserve, to a great extent, the local behavior of α, z_{rev}, and $w(z_{rev})$. Larger deviations from the parent quantities typically are in regions of very small densities, mostly off the ends of the molecules. Such deviations are inconsequential, since the roles of α and z_{rev} are to distinguish chemically distinct regions and w switches between them.

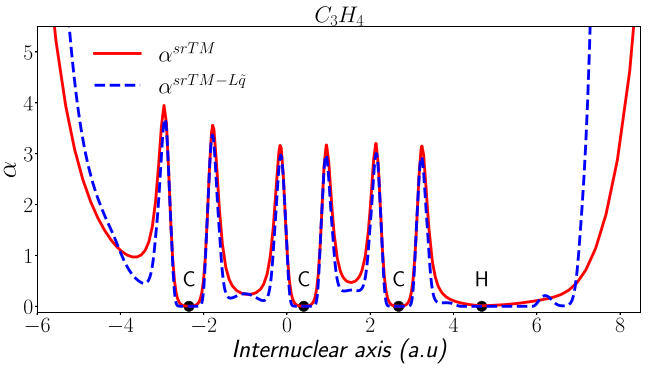

Figure 7. As in Figure 3 but for the C_3H_4 molecule.

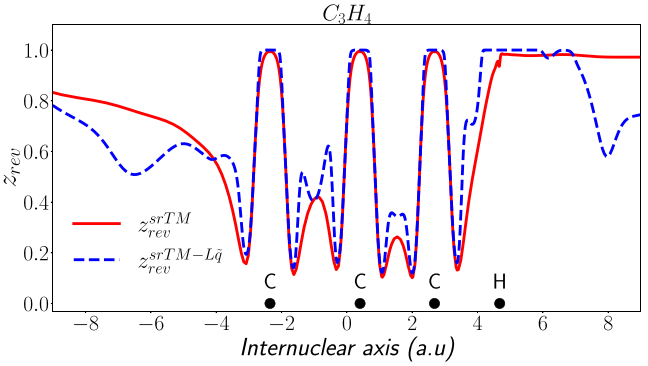

Figure 8. As in Figure 4 but for the C_3H_4 molecule.

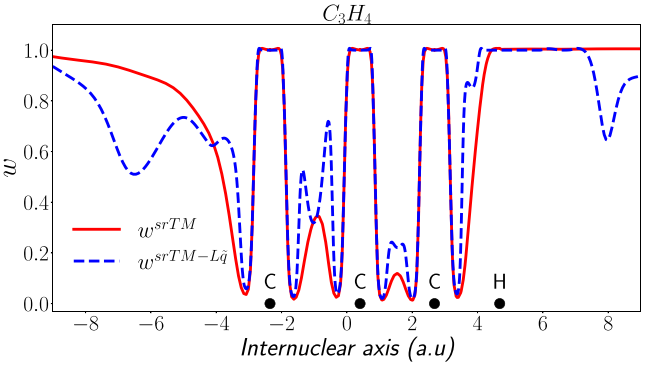

Figure 9. As in Figure 5 but for the C_3H_4 molecule.

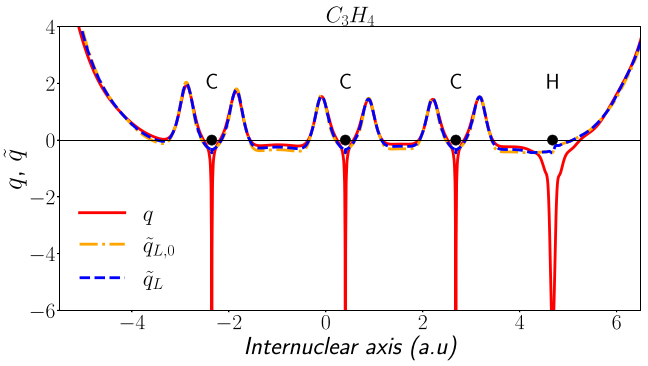

Figure 10. As in Figure 6 but for the C_3H_4 molecule.

https://doi.org/10.1021/acs.jpca.4c02635
J. Phys. Chem. A 2024, 128, 6010−6018

The remaining physical property comparison is elemental 3d magnetization. Figures 11, 12, and 13 show the fixed spin moment energy as a function of magnetization for bcc Fe, fcc Co, and fcc Ni as calculated from the PBE,[25] *sr*TM, *sr*TM-L_{MRT}, and *sr*TM-L$\tilde{q}$ functionals. For the *sr*TM-L$\tilde{q}$, the PC_{opt}, Scheme 1 version was used, since it is superior on MADs. Table 7 gives the saturation magnetizations. In two cases, the deorbitalization from *sr*TM to *sr*TM-L$\tilde{q}$ sustains or slightly alters the saturation magnetization. For Fe, it is a small underestimate, but there is a small overestimate for Co. For these two, the new deorbitalization preserves the elemental magnetization properties of its parent *sr*TM orbital-dependent functional. [Aside, by inference it also preserves the performance of the antecedent version of TM, *rreg*TM that was the original motivation; see Paper I.] The Ni case is a bit poorer.

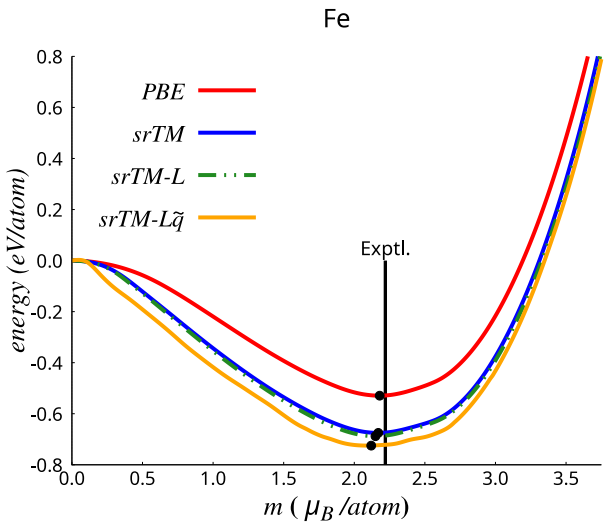

Figure 11. Fixed spin moment energy on a per-atom basis for bcc Fe from four XC functionals using the calculated equilibrium lattice parameters.

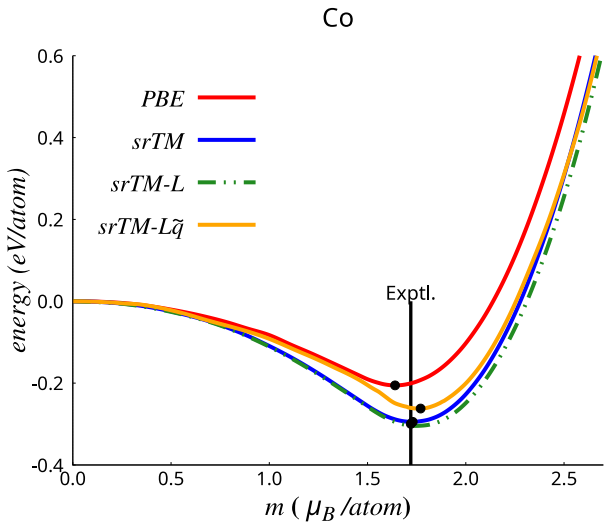

Figure 12. As in Figure 11 for fcc Co.

Regarding computational performance, Table 8 displays the total time, the number of SCF steps, and the total time per SCF step for the six-molecule test set AE6.[28] We use it as a reasonable sample of different bonding types. It is evident that, across all the deorbitalized versions done with a $\tilde{q}$ scheme, there is a slight increase in the total time compared to the original deorbitalization of *v2-sreg*TM (recall Paper II). However, conversely, the number of SCF steps for all versions is slightly lower compared to that earlier deorbitalization.

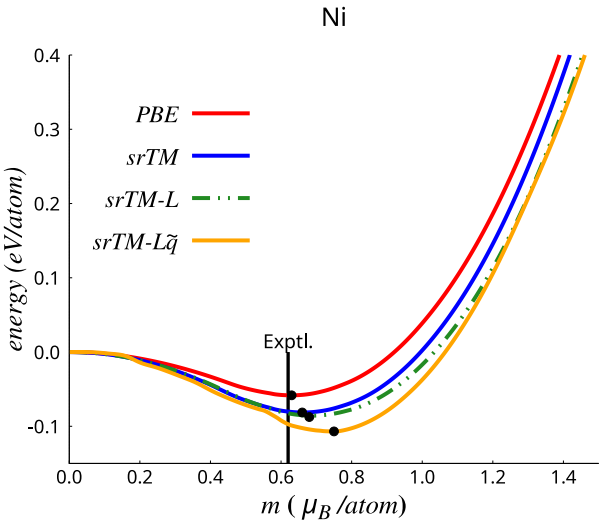

Figure 13. As in Figure 11 for fcc Ni.

Table 7. Magnetic Moments in μ_B for Three Elemental 3d Solids as Determined from Different XC Functionals[a]

	Exp.	PBE	*sr*TM	*sr*TM-L	*sr*TM-L$\tilde{q}$
Fe	2.22	2.18	2.17	2.15	2.12
Co	1.72	1.64	1.73	1.75	1.77
Ni	0.62	0.63	0.66	0.69	0.75

[a]Exp. refers to the experimental data.[26,27]

SUMMARY

By extension of the M-RT strategy to involve use of a recursively smoothed version $\tilde{q}_L$ of the reduced density Laplacian q instead of q itself, we have produced a successful deorbitalization of the simplified, regularized Tao−Mo exchange−correlation functional *srTM* (denoted in preceding papers as *v2-sregTM*). Detailed examination of two schemes with each of two deorbitalizers leads to the recommendation to use PC_{opt} with Scheme 1.

The recommended deorbitalized functional matches or exceeds the accuracy of the parent functional on standard molecular and solid test sets (except for bulk moduli), preserves most of the elemental 3d magnetization, and reproduces the orbital-dependent chemical indicator functions α and z_{rev} and the switching function $w(z_{rev})$ in important bonding regions.

This advance resolves the puzzling and somewhat unsatisfactory mixed outcome of the previous deorbitalization.[2] More broadly, it generalizes and extends the M-RT deorbitalization strategy beyond simple substitution of KEDFs for the Kohn−Sham kinetic energy density. The analysis leading to the $\tilde{q}_L$ strategy also led, along the way, to insight as to why the "brutal approximation" of Paper II actually worked to the extent that it did.

We remark that the recursive $\tilde{q}_L(q)$ is not expected to improve deorbitalization of functionals such as MVS,[29] SCAN,[30,31] or r^{2}SCAN.[24] They depend only on α, for which

https://doi.org/10.1021/acs.jpca.4c02635
J. Phys. Chem. A 2024, 128, 6010−6018

Table 8. Total Timings, Number of SCF Steps, and Times per SCF Step Calculated for Each Molecule from the Molecular Test Set AE6

				*sr*TM-L$\tilde{q}$			
		*sr*TM[1]	*sr*TM-L[2]	PC_{rep}		PC_{opt}	
			$PC_{rep}(p,q)$	Scheme 1	Scheme 2	Scheme 1	Scheme 2
SiH_4	Total time (*s*)	4.3	4.8	5.1	5.2	4.1	4.1
	Total steps	6	7	7	7	6	6
	Time/step	0.72	0.69	0.73	0.74	0.68	0.68
SiO	Total time (*s*)	2.5	2.7	3.0	2.2	2.6	3.5
	Total steps	9	9	8	8	9	9
	Time/step	0.28	0.30	0.38	0.28	0.29	0.39
S_2	Total time (*s*)	4.0	4.7	4.4	4.0	3.6	3.6
	Total steps	7	9	8	8	7	7
	Time/step	0.57	0.52	0.55	0.50	0.51	0.51
C_3H_4 (propyne)	Total time (*s*)	12.7	15.1	14.1	14.1	15.6	15.3
	Total steps	7	9	8	8	9	9
	Time/step	1.81	1.68	1.76	1.76	1.73	1.70
$C_2H_2O_2$ (glyoxal)	Total time (*s*)	10.6	13.2	13.4	12.5	11.9	11.7
	Total steps	7	9	8	8	8	8
	Time/step	1.51	1.47	1.68	1.56	1.49	1.46
C_4H_8 (cyclobutane)	Total time (*s*)	33.6	45.1	51.7	50.9	50.3	51.1
	Total steps	6	8	9	9	9	9
	Time/step	5.60	5.64	5.74	5.66	5.59	5.68
Complete AE6	Total time (*s*)	67.7	85.6	91.7	88.9	88.1	89.3
	Total steps	42	51	48	48	48	48

the M-RT strategy already has been shown to be satisfactory. This is confirmed by calculation. For r^{2}SCAN-L$\tilde{q}$ versus original M-RT r^{2}SCAN-L,[6] both with PC_{opt}, the molecular heat of formation MAD is worsened drastically, 16.05 kcal/mol versus 5.30 kcal/mol. The bond length and frequency MADs are much closer, respectively 0.009 Å versus 0.011 Å and 27.78 cm^{-1} versus 25.6 cm^{-1}. The comparison of heat of formation MADs is even worse for CR_{opt} deorbitalization of the MVS.[29] The original M-RT result is 6.20 kcal/mol[3] versus 29.757 kcal/mol for MVS-L$\tilde{q}$ Scheme 1. These results are consistent with ordinary expectations. Introduction of an extra approximation to an already successful deorbitalization would seem almost certain to worsen the results.

■ ASSOCIATED CONTENT

Supporting Information

The following file is available free of charge. The Supporting Information is available free of charge at https://pubs.acs.org/doi/10.1021/acs.jpca.4c02635.

Detailed, system-by-system tabulation of the numerical results of the test calculations against standard molecular and solids (enthalpies, bond lengths, vibrational frequencies, band gaps, lattice constants, energies, moduli) and detailed results on 3d elemental magnetization (PDF)

■ AUTHOR INFORMATION

Corresponding Authors

H. Francisco − *Quantum Theory Project, Department of Physics, University of Florida, Gainesville, Florida 32611, United States;* orcid.org/0000-0001-6163-8436; Email: francisco.hector@ufl.edu

S. B. Trickey − *Quantum Theory Project, Department of Physics and Department of Chemistry, University of Florida, Gainesville, Florida 32611, United States;* orcid.org/0000-0001-9224-6304; Email: trickey@ufl.edu

Author

A. C. Cancio − *Department of Physics and Astronomy, Ball State University, Muncie, Indiana 47306, United States*

Complete contact information is available at: https://pubs.acs.org/10.1021/acs.jpca.4c02635

Notes

The authors declare no competing financial interest.

■ ACKNOWLEDGMENTS

Work supported by U.S. National Science Foundation grant DMR-1912618.

■ REFERENCES

(1) Francisco, H.; Cancio, A. C.; Trickey, S. B. Reworking the Tao−Mo exchange−correlation functional. I. Reconsideration and simplification. *J. Chem. Phys.* **2023**, *159*, 214102.

(2) Francisco, H.; Cancio, A. C.; Trickey, S. B. Reworking the Tao−Mo exchange-correlation functional. II. De-orbitalization. *J. Chem. Phys.* **2023**, *159*, 214103.

(3) Mejía-Rodríguez, D.; Trickey, S. B. Deorbitalization strategies for meta-generalized-gradient-approximation exchange-correlation functionals. *Phys. Rev. A* **2017**, *96*, 052512.

(4) Mejía-Rodríguez, D.; Trickey, S. B. Deorbitalized meta-GGA exchange-correlation functionals in solids. *Phys. Rev. B* **2018**, *98*, 115161.

(5) Oliver, G. L.; Perdew, J. P. Spin-Density Gradient Expansion of the Kinetic Energy. *Phys. Rev. A* **1979**, *20*, 397−403.

(6) Mejía-Rodríguez, D.; Trickey, S. B. Meta-GGA performance in solids at almost GGA cost. *Phys. Rev. B* **2020**, *102*, 121109.

(7) Tao, J.; Mo, Y. Accurate Semilocal Density Functional for Condensed-Matter Physics and Quantum Chemistry. *Phys. Rev. Lett.* **2016**, *117*, 073001.

(8) Jana, S.; Sharma, K.; Samal, P. Improving the Performance of Tao−Mo Non-empirical Density Functional with Broader Applicability in Quantum Chemistry and Materials Science. *J. Phys. Chem. A* **2019**, *123*, 6356−6369.
(9) Patra, A.; Jana, S.; Samal, P. A way of resolving the order-of-limit problem of Tao−Mo semilocal functional. *J. Chem. Phys.* **2020**, *153*, 184112.
(10) Jana, S.; Behera, S. K.; Śmiga, S.; Constantin, L. A.; Samal, P. Accurate density functional made more versatile. *J. Chem. Phys.* **2021**, *155*, 024103.
(11) Curtiss, L. A.; Raghavachari, K.; Redfern, P. C.; Pople, J. A. Assessment of Gaussian-2 and density functional theories for the computation of enthalpies of formation. *J. Chem. Phys.* **1997**, *106*, 1063−1079.
(12) Curtiss, L. A.; Redfern, P. C.; Raghavachari, K.; Pople, J. A. Gaussian-3X (G3X) theory: Use of improved geometries, zero-point energies, and Hartree−Fock basis sets. *J. Chem. Phys.* **2001**, *114*, 108−117.
(13) Perdew, J. P.; Constantin, L. A. Laplacian-level density functionals for the kinetic energy density and exchange-correlation energy. *Phys. Rev. B* **2007**, *75*, 155109.
(14) Staroverov, V. N.; Scuseria, G. E.; Tao, J.; Perdew, J. P. Comparative assessment of a new nonempirical density functional: Molecules and hydrogen-bonded complexes. *J. Chem. Phys.* **2003**, *119*, 12129−12137.
(15) Staroverov, V. N.; Scuseria, G. E.; Tao, J.; Perdew, J. P. Erratum: Comparative assessment of a new nonempirical density functional: Molecules and hydrogen-bonded complexes [J. Chem. Phys. 119, 12129 (2003)]. *J. Chem. Phys.* **2004**, *121*, 11507−11507.
(16) Peng, H.; Yang, Z.-H.; Perdew, J. P.; Sun, J. Versatile van der Waals Density Functional Based on a Meta-Generalized Gradient Approximation. *Phys. Rev. X* **2016**, *6*, 041005.
(17) Tran, F.; Stelzl, J.; Blaha, P. Rungs 1 to 4 of DFT Jacob's ladder: Extensive test on the lattice constant, bulk modulus, and cohesive energy of solids. *J. Chem. Phys.* **2016**, *144*, 204120.
(18) Tran, F.; Blaha, P. Importance of the Kinetic Energy Density for Band Gap Calculations in Solids with Density Functional Theory. *J. Phys. Chem. A* **2017**, *121*, 3318−3325.
(19) Mi, W.; Luo, K.; Trickey, S. B.; Pavanello, M. Orbital-Free Density Functional Theory: An Attractive Electronic Structure Method for Large-Scale First-Principles Simulations. *Chem. Rev.* **2023**, *123*, 12039−12104.
(20) Kato, T. On the Eigenfunctions of Many-particle Systems in Quantum Mechanics. *Commun. Pure. Appl. Math.* **1957**, *10*, 151−177.
(21) Bingel, W. The Behaviour of the First-order Density Matrix at the Coulomb Singularities of the Schrödinger Equation. *Z. Naturforschung A* **1963**, *18*, 1249−1253.
(22) Pack, R.; Brown, W. Cusp Conditions for Molecular Wave Functions. *J. Chem. Phys.* **1966**, *45*, 556−559.
(23) March, N.; Howard, I. A.; Holas, A.; Senet, P.; Van Doren, V. Nuclear Cusp Conditions for Components of the Molecular Energy Relevant for Density Functional Theory. *Phys. Rev. A* **2000**, *63*, 012520.
(24) Furness, J. W.; Kaplan, A. D.; Ning, J.; Perdew, J. P.; Sun, J. Accurate and Numerically Efficient r^2SCAN Meta-Generalized Gradient Approximation. *J. Phys. Chem. Lett.* **2020**, *11*, 8208−8215.
(25) Perdew, J. P.; Burke, K.; Ernzerhof, M. Generalized Gradient Approximation Made Simple. *Phys. Rev. Lett.* **1996**, *77*, 3865−3868.
(26) Danan, H.; Herr, A.; Meyer, A. J. P. New Determinations of the Saturation Magnetization of Nickel and Iron. *J. Appl. Phys.* **1968**, *39*, 669−670.
(27) Myers, H. P.; Sucksmith, W. The spontaneous magnetization of cobalt. *Proc. R. Soc. A* **1951**, *207* (1091), 427−446.
(28) Lynch, B. J.; Truhlar, D. G. Small Representative Benchmarks for Thermochemical Calculations. *J. Phys. Chem. A* **2003**, *107*, 8996−8999.
(29) Sun, J.; Perdew, J. P.; Ruzsinszky, A. Semilocal density functional obeying a strongly tightened bound for exchange. *Proc. Nat. Acad. Sci. (USA)* **2015**, *112*, 685−689.
(30) Sun, J.; Ruzsinszky, A.; Perdew, J. P. Strongly Constrained and Appropriately Normed Semilocal Density Functional. *Phys. Rev. Lett.* **2015**, *115*, 036402.
(31) Sun, J.; Remsing, R. C.; Zhang, Y.; Sun, Z.; Ruzsinszky, A.; Peng, H.; Yang, Z.; Paul, A.; Waghmare, U.; Wu, X.; et al. Accurate first-principles structures and energies of diversely bonded systems from an efficient density functional. *Nat. Chem.* **2016**, *8*, 831−836.

https://doi.org/10.1021/acs.jpca.4c02635
J. Phys. Chem. A 2024, 128, 6010−6018